Biogeosciences, 7, 3783–3797, 2010
www.biogeosciences.net/7/3783/2010/
doi:10.5194/bg-7-3783-2010

Biogeosciences

Phytoplankton-bacteria coupling under elevated CO_2 levels: a stable isotope labelling study

A. de Kluijver[1], K. Soetaert[1], K. G. Schulz[2], U. Riebesell[2], R. G. J. Bellerby[3,4], and J. J. Middelburg[1,5]

[1]Netherlands Institute of Ecology (NIOO-KNAW), Centre for Estuarine and Marine Ecology, P.O. Box 140, 4400 AC Yerseke, The Netherlands
[2]Leibniz Institute for Marine Sciences (IFM-GEOMAR), Düsternbrooker Weg 20, 24105 Kiel, Germany
[3]Bjerknes Centre for Climate Research, University of Bergen, Allégaten 55, 5007 Bergen, Norway
[4]Geophysical Institute, University of Bergen, Allégaten 70, 5007 Bergen, Norway
[5]Faculty of Geosciences, Utrecht University, P.O. Box 80021, 3508 TA Utrecht, The Netherlands

Received: 13 April 2010 – Published in Biogeosciences Discuss.: 6 May 2010
Revised: 5 November 2010 – Accepted: 8 November 2010 – Published: 24 November 2010

Abstract. The potential impact of rising carbon dioxide (CO_2) on carbon transfer from phytoplankton to bacteria was investigated during the 2005 PeECE III mesocosm study in Bergen, Norway. Sets of mesocosms, in which a phytoplankton bloom was induced by nutrient addition, were incubated under 1× (∼350 µatm), 2× (∼700 µatm), and 3× present day CO_2 (∼1050 µatm) initial seawater and sustained atmospheric CO_2 levels for 3 weeks. ^{13}C labelled bicarbonate was added to all mesocosms to follow the transfer of carbon from dissolved inorganic carbon (DIC) into phytoplankton and subsequently heterotrophic bacteria, and settling particles. Isotope ratios of polar-lipid-derived fatty acids (PLFA) were used to infer the biomass and production of phytoplankton and bacteria. Phytoplankton PLFA were enriched within one day after label addition, whilst it took another 3 days before bacteria showed substantial enrichment. Group-specific primary production measurements revealed that coccolithophores showed higher primary production than green algae and diatoms. Elevated CO_2 had a significant positive effect on post-bloom biomass of green algae, diatoms, and bacteria. A simple model based on measured isotope ratios of phytoplankton and bacteria revealed that CO_2 had no significant effect on the carbon transfer efficiency from phytoplankton to bacteria during the bloom. There was no indication of CO_2 effects on enhanced settling based on isotope mixing models during the phytoplankton bloom, but this could not be determined in the post-bloom phase. Our results suggest that CO_2 effects are most pronounced in the post-bloom phase, under nutrient limitation.

Correspondence to: A. de Kluijver
(a.dekluijver@nioo.knaw.nl)

1 Introduction

The ocean is one of the largest reservoirs of CO_2 on earth and one of the largest sinks for anthropogenic CO_2 emissions (Sabine et al., 2004). The biologically mediated flux of CO_2 into the oceans, called the biological pump, is the transport of organic matter (OM) produced at the oceans' surface to the ocean interior, sustaining a vertical CO_2 gradient. The strength of the biological pump is largely controlled by three processes: primary production, community respiration and the export rate of particulate organic matter (POM) into the deep ocean. Community respiration in the euphotic zone, dominated by heterotrophic bacteria, converts organic carbon back into CO_2 and thus decreases the oceans' CO_2 uptake capacity (Rivkin and Legendre, 2001). The coupling between phytoplankton and heterotrophic bacteria is mainly via labile dissolved organic matter (DOM). In the upper ocean an important source for labile DOM and subsequently for heterotrophic bacteria is the release of carbon-rich substances by phytoplankton, further referred to as exudation (Larsson and Hagström, 1979). Phytoplankton exudation has been defined as the release of excess photosynthates that accumulate when carbon fixation exceeds incorporation into new cell material (Fogg, 1983). The rate of exudation is linked to primary production and is highest under nutrient-poor conditions, when

nutrient limitation impedes phytoplankton growth, but not photosynthetic carbon fixation (Fogg, 1983). Changes in primary production can potentially alter exudation and subsequently phytoplankton-bacteria coupling and the microbial food-web. Increasing CO_2 levels could stimulate primary production (Riebesell et al., 1993), which could result in an increased flow of inorganic carbon into carbon exudates. Carbon exudates tend to accrete into transparent exopolymer particles (TEP), which facilitate aggregation due to their sticky nature (Engel et al., 2004b). These aggregates can facilitate carbon export to the deep ocean if the carbon is not remineralised (Fig. 1).

Increased inorganic carbon consumption relative to nitrogen uptake at higher CO_2 levels was observed in natural plankton communities (Riebesell et al., 2007; Bellerby et al., 2008). The additional community uptake of CO_2, however, was not reflected in higher standing stocks of organic material in the surface layer (Fig. 1) (Riebesell et al., 2007; Schulz et al., 2008; Egge et al., 2009). Although carbon export could not be quantified directly, the authors proposed that the extra carbon was released as exudates that coalesced and sank to the deep (Fig. 1). This implies that increasing CO_2 concentrations could strengthen the biological pump and in this way act as a negative feedback on increasing atmospheric CO_2 concentrations (Arrigo, 2007). However, this requires that the additional organic material escapes remineralisation by heterotrophic bacteria in the upper layer, which could not be quantified. The community uptake did not account for carbon flows in and from phytoplankton to bacteria to separate primary production from remineralisation (Fig. 1).

Traditionally, the carbon coupling between phytoplankton and bacteria is derived from the relationship between production and abundance of phytoplankton and bacteria (Cole et al., 1988). The drawback of these methods is that net processes are measured and that temporal and spatial decoupling and grazing cannot be quantified. The use of carbon isotope tracers (^{13}C, ^{14}C) provides the possibility to directly quantify the flux of carbon from dissolved inorganic carbon (DIC) to phytoplankton and subsequently bacteria and this method has been successfully used in previous mesocosm experiments (Norrman et al., 1995; Lyche et al., 1996) and in whole lake isotope tracer addition experiments (Kritzberg et al., 2004; Pace et al., 2007). Since it is difficult to physically separate phytoplankton from bulk particulate organic matter (POM), the isotope signal of POM has often been used as a representative for phytoplankton, which can lead to an underestimation of phytoplankton carbon uptake. Similar methodological limitations exist to determine the bacteria isotope signature. A valuable alternative is the analysis of isotope label in biomarkers specific for bacteria and phytoplankton groups (polar-lipid-derived fatty acids, PLFA). The combined technique of isotope labelling and biomarker analysis has proven a very powerful tool to study carbon flows in natural communities, especially in perturbation experiments (Boschker and Middelburg, 2002; Van Den Meersche et al., 2004; Pace et al., 2007). Furthermore, label incorporation into phytoplankton biomarkers can be used to determine group-specific growth-rates (Dijkman et al., 2009). Here, we applied the isotope labelling technique to quantify phytoplankton-bacteria coupling under different CO_2 levels. More specifically, we address potential effects of CO_2 on phytoplankton production and growth, and transfer of freshly produced organic matter to the microbial food web and into settling particles (Fig. 1). The results contribute to the previous published results on PeECE III by unravelling the carbon interactions between the major planktonic food-web compartments.

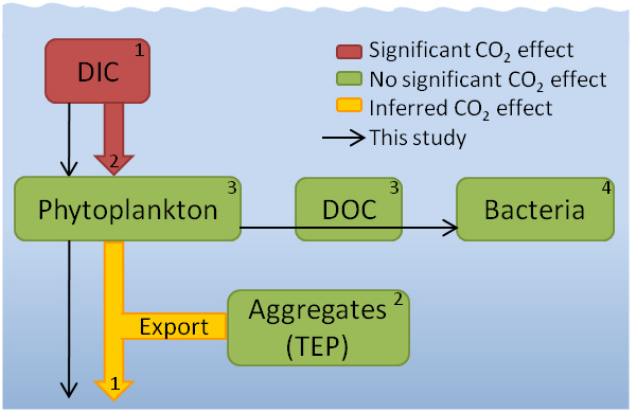

Fig. 1. Carbon fluxes between the major food-web compartments of this study and the previous published CO_2 effect on these compartments and fluxes in the PeECE III 2005 mesocosm study. [1]Riebesell et al. (2007) found increased cumulative DIC drawdown at increased pCO_2 during the bloom and inferred enhanced export at high pCO_2; [2]Egge et al. (2008) demonstrated increased cumulative ^{14}C incorporation at higher pCO_2 in the post-bloom phase; [3]Schulz et al. (2008); [4]Allgaier et al. (2008).

2 Material and methods

2.1 Set-up and sampling

The PeECE III mesocosm experiment was carried out at the Marine Biological Station, University of Bergen, Norway, between 16 May and 10 June 2005. Nine mesocosms (M1 to M9) of 9.5 m deep and with a volume of 27 m^3 each were filled with unfiltered, nutrient-poor post-bloom water from the fjord, and manipulated to achieve 3 sets of different CO_2 levels in mesocosms by aeration of the water column and the overlying atmosphere with CO_2-enriched air. The partial pressures of carbon dioxide (pCO_2) at the start of the experiment were about 350 µatm (1× CO_2, M7–9), 700 µatm (2× CO_2, M4–6), and 1050 µatm (3× CO_2, M1–3). These concentrations are expected during to happen during the first half and towards the end of this century under a business-as-usual CO_2 emission scenario. Nitrate (final

concentration 15 µmol l^{-1}) and phosphate (final concentration 0.7 µmol l^{-1}) were added to the mesocosms to initiate a phytoplankton bloom. A more detailed description of the experimental set-up can be found in (Schulz et al., 2008). ^{13}C-labeled bicarbonate was added to the upper 5 m of the mesocosms between day 0 and day 1 to a final addition of ca 2.3 µmol kg^{-1}, corresponding to about 0.1% of total DIC. Water samples for polar lipid fatty acids (PLFA) were taken from the upper layer of each mesocosm daily (day 0–18) or every second day (day 20, 22 and 24). The samples were filtered on pre-combusted GF/F filters and stored frozen until further analysis. Sediment traps were placed in each mesocosm at 7.5 m depth and they were collected every 3 days, on day 4, 7, 10, 13, 16, and 19.

2.2 PLFA and DIC analysis

The lipids were extracted by a modified Bligh and Dyer method (Bligh and Dyer, 1959; Boschker et al., 1998). The lipids were fractionated in different polarity classes by column separation on a heat-activated-silicic acid column and subsequent elution with chloroform, acetone and methanol. The methanol fractions, containing most of the polar-lipid fatty acids, were derivatised to fatty acid methyl esters (FAME). The standards 12:0 and 19:0 were used as internal standards. PLFA concentrations were determined by gas chromatograph-flame ionization detection (GC-FID). The δ^{13}C of individual PLFA were measured using gas chromatography-combustion isotope ratio mass spectrometry (GC-C-IRMS (Middelburg et al., 2000; Van Den Meersche et al., 2004). DIC was analyzed by coulometric titration (Bellerby et al., 2008) and its isotope ratio by a Finnigan GasBench coupled to a Mat 252 mass spectrometer.

2.3 Data analysis

Stable isotope data are expressed in the delta notation (δ^{13}C) relative to VPDB standard and the ^{13}C fraction ($^{13}C/(^{12}C+^{13}C)) = {}^{13}r$ was derived from the delta notation. Total amount of labelled biomass (total ^{13}C) is calculated as

$$\text{total}^{13}\text{C} = ({}^{13}r_{\text{sample}} - {}^{13}r_{\text{control}}) \cdot \text{concentration (µgC l}^{-1}) \quad (1)$$

where $^{13}C_{control}$ is the isotope fraction at day 0, see Middelburg et al. (2000) and Van Den Meersche et al. (2004) for details. To be able to directly compare labelling of phytoplankton and bacteria biomass between the different mesocosms, the data were corrected for small differences in initial ^{13}C-DIC concentrations. This correction factor was calculated for each mesocosm as total ^{13}C-DIC at day 1 relative to the average total ^{13}C-DIC of all mesocosms at day 1. The correction factor ranged from 0.75 to 1.09.

Out-gassing of ^{13}C-DIC was calculated according to Delille et al. (2005) with chemical enhancement factors. The concentration of $^{13}CO_2$ (aq) was derived from ^{13}C-DIC as described in Zeebe and Wolf-Gladrow (2001) with fractionation factors from Zhang et al. (1995) with CO_2 concentrations measured by Bellerby et al. (2008). An approximation of δCO_2-air of −8‰ was used, because no exact measures were available (Fry, 2006).

The sum of PLFA ai15:0 and i15:0 was used to characterize heterotrophic (gram-positive) bacteria and in the section on methodological comparison, the PLFA 18:1ω7c (gram-negative bacteria) was included. The sum of PLFA 22:6ω3, 20:5ω3, 18:4ω3, 18:5(*n*-3, 6, 9, 12, 16), 18:5ω3, and 18:3ω3 were used to characterize phytoplankton dynamics (Boschker and Middelburg, 2002; Dijkman and Kromkamp, 2006; Dijkman et al., 2009). Phytoplankton communities were further divided into diatoms (PLFA 16:2ω4, 16:4ω1 and 20:5ω3), coccolithophores (PLFA 18:5ω3 and 18:5(*n*-3, 6, 9, 12, 16)), and green algae (16:4ω3 and 18:3ω3) (Dijkman and Kromkamp, 2006; Dijkman et al., 2009). Phytoplankton composition based on PLFA was also estimated with the Bayesian compositional estimator (Van Den Meersche et al., 2008) with the input ratio from (Dijkman and Kromkamp, 2006). The final step involved conversion from PLFA to cell biomass. Bacterial biomass was calculated using a conversion factor of 0.0059 g C (ai+i)15:0 per g C biomass, which is the product of 0.056 g C PLFA per g C biomass (Brinch Iversen and King, 1990; Middelburg et al., 2000) and 0.105 g C ai15:0+i15:0 per g C PLFA (calculated from Boschker et al., 1998 and references cited therein). Calculated in the same way, the sum of ai15:0+i15:0+18:1ω7c encompassed 25% of PLFA and the final conversion factor was 0.0137 g C (ai+i15:0, 18:1ω7c) per g C biomass. We used a carbon content of 20 fg $cell^{-1}$ to convert bacterial biomass to cells (Lee and Fuhrman, 1987). The conversion factors for phytoplankton (groups) were derived from data on fatty acid composition in (Dijkman and Kromkamp, 2006). Chlorophyll-*a* (chl-*a*) concentrations were converted to biomass assuming a C to chl-*a* ratio of 45 based on literature values. Although conversion factors are disputable, they do not affect the general patterns nor inferred transfer dynamics from phytoplankton to bacteria. Group-specific growth rates (µ, d^{-1}) during the bloom (from day 5 to day 9) were calculated as

$$\mu = \ln \frac{^{13}\text{C biomass}_{t+\Delta t}}{^{13}\text{C biomass}_{t}} / \Delta t \quad (2)$$

Data from sediment traps were only analyzed for isotope ratios of specific PLFA and not for concentrations because these were biased due to significant over trapping (Schulz et al., 2008). The material in the traps was subdivided in phytoplankton and bacteria using PLFA, similarly as for the suspended particulate matter. The fraction of material derived from the upper layer in the settled material was calculated with the mixing equation (Fry, 2006). The equation used is:

$$f_{\text{upper layer}} = \left(\delta^{13}\text{C}_{\text{sediment}} - \delta^{13}\text{C}_{\text{control}}\right) / \left(\delta^{13}\text{C}_{\text{upper layer}} - \delta^{13}\text{C}_{\text{control}}\right) \quad (3)$$

where $\delta^{13}C_{control}$ is the isotope ratio at day 0 and $\delta^{13}C_{upper\ layer}$ is the isotope ratio of the pelagic PLFA, averaged over the days of settlement. This fraction provides a measure of exchange between upper and deeper layer and can therefore be used as an indication of sinking.

Within the PeECE III study, POC, inorganic nutrients, and chl-*a* (Schulz et al., 2008), pigments (Riebesell et al., 2007; Schulz et al., 2008), and bacterial numbers (Allgaier et al., 2008; Paulino et al., 2008) were published earlier and used for comparative purposes in this study.

2.4 Model

A simple source-sink isotope ratio model was used to determine label transfer from phytoplankton to bacteria (Hamilton et al., 2004; Van Oevelen et al., 2006). The following equation was used

$$\frac{d\delta^{13}C_{bac}}{dt} = r_{bac} \cdot f_{phyto} \cdot \delta^{13}C_{phyto} - r_{bac} \cdot \delta^{13}C_{bac} \quad (4)$$

where r_{bac} = bacteria turnover (d^{-1}) and f_{phyto} = fraction of ^{13}C derived from phytoplankton.

The weighted $\Delta\delta^{13}C$ of phytoplankton was used as a forcing function and the weighted $\Delta\delta^{13}C$ of bacteria was used for model calibration. The original data were used to fit the model, instead of ^{13}C-DIC normalized data, but they would give similar results. The assumption for this model is that biomass is constant with time. The model equations were implemented in R, using the packages FME and deSolve (Soetaert and Petzoldt, 2009; Soetaert et al., 2009).

The time sequence of the model was 0–24 days and initial conditions were set to 0. Parameter calibration was done with pseudo-randomization followed by Levenberg-Marquardt algorithm (Press et al., 2001). The parameters were further assessed with the Markov-Chain-Monte-Carlo technique (MCMC) (Gelman et al., 1996). During the MCMC, the model was run 5000 times for each mesocosm, resulting in approximately 1500–1750 accepted runs per mesocosm. The mean and standard deviation were calculated for each parameter.

The dependency of heterotrophic bacteria on recently fixed carbon was also calculated using mean isotope ratios over the last 10 days of the experiment ($\Delta\delta^{13}C_{bac}/\Delta\delta^{13}C_{phyto}$). This simple calculated ratio should approach f_{phyto} at steady-state (Van Oevelen et al., 2006).

2.5 Statistics

Results are reported as mean ± standard deviation. In order to test if measured concentrations of phytoplankton and bacteria differed significantly ($p < 0.05$) over time among pCO_2 levels, repeated measures ANOVAs and Bonferroni post-hoc tests were applied using the software Statistica® (stat Soft, Inc., US, 2009). Prior to analyses, data were checked for normality, homogeneity of variance, and sphericity. Significant ($p < 0.05$) differences in phytoplankton growth rates and model parameters were assessed using one-way ANOVA.

3 Results

3.1 Phytoplankton dynamics

PLFA specific for phytoplankton were used to depict phytoplankton dynamics and their carbon concentrations were converted to total carbon biomass. The addition of nutrients induced a phytoplankton bloom as depicted by both PLFA (Fig. 2a) and chlorophyll-*a* (Fig. 2b). During the experiment 3 different phases in phytoplankton dynamics could be observed: before the bloom (day 0–5), the bloom (day 5–9), and the post bloom (after day 9). Based on nutrient dynamics, 4 phases were identified by Riebesell et al. (2008) and Tanaka et al. (2008). From start until day 6, there was no nutrient depletion, during day 7–9 silicate was depleted, during day 10–12 silicate and phosphate were depleted and from day 13 onwards, all nutrients were depleted. The development of the bloom as depicted by PLFA reflects the dynamics of phosphate concentrations. When phosphate became depleted, the phytoplankton bloom collapsed (Fig. 2a, h). Phytoplankton biomass (based on PLFA) was low in the first five days of the experiment, with values $<0.2\,mg\,C\,L^{-1}$. After day 5 the phytoplankton bloom started and phytoplankton biomass rapidly increased up to $0.71 \pm 0.10\,mg\,C\,L^{-1}$ at day 9, the peak of the bloom assessed using PLFA (Fig. 2a). The bloom collapsed after day 9 to $0.16 \pm 0.043\,mg\,C\,L^{-1}$ at day 10 and stayed around this concentration until the end of the experiment. Phytoplankton biomass (based on chl-*a*) increased from $0.064 \pm 0.0091\,mg\,C\,L^{-1}$ at day 0 to $0.55 \pm 0.11\,mg\,C\,L^{-1}$ at day 10, the peak of the bloom. From then on, the bloom continuously decreased until starting values were reached again around day 16 (Fig. 2b) (Schulz et al., 2008).

No CO_2 effects on phytoplankton concentrations and dynamics were observed before and during the bloom (day 0–9). During the post-bloom the phytoplankton biomass based on PLFA was significantly lower in the $1\times CO_2$ treatment than in the $2\times$ and $3\times CO_2$ treatments (repeated measures ANOVA, $F\ (2,6) = 25.66$, $p < 0.005$) (Table 1). The largest differences in biomass occurred between day 12 and day 17. The development of phytoplankton biomass as determined with PLFA (Fig. 2a), chl-*a* (Fig. 2b) and particulate organic carbon (POC) are summarized in Fig. 3a. The range in biomass is similar for all methods, with values from 0–$1.2\,mg\,C\,L^{-1}$. The timing of the bloom, however, is different for all methods. The peak of the bloom was at day 9 with PLFA, at day 10 with chl-*a*, and at day 11 for POC.

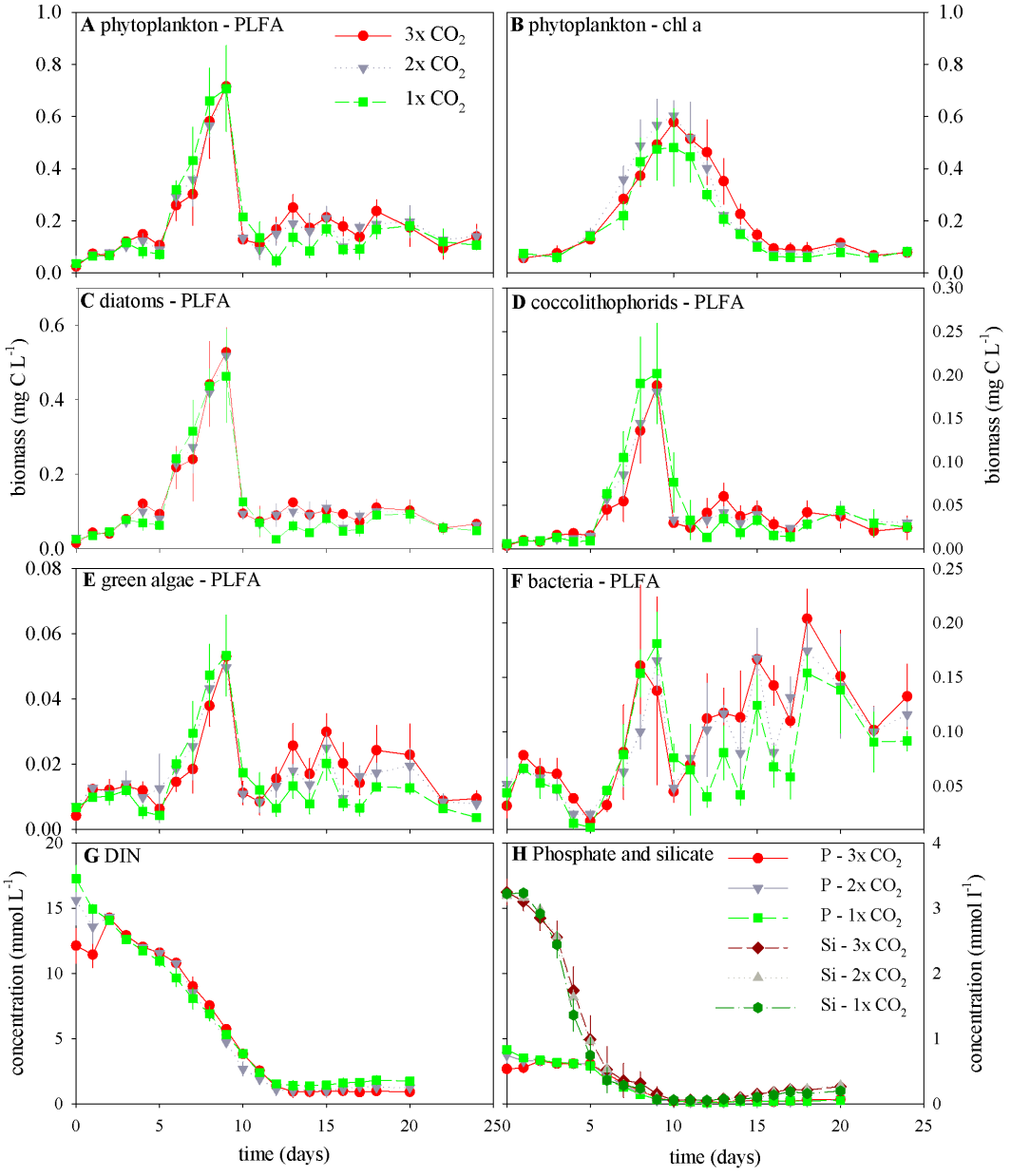

Fig. 2. Concentrations of **(A)** total phytoplankton carbon based on PLFA, **(B)** total phytoplankton carbon based on chlorophyll-*a* and PLFA derived carbon estimates for **(C)** diatoms, **(D)** coccolithophores, **(E)** green algae, **(F)** bacteria. Concentrations of **(G)** dissolved inorganic nitrogen, **(H)** phosphate and silicate in the different CO_2 treatments. Average and SD of the three replicates are shown.

Phytoplankton was further subdivided into the major phytoplankton groups. Conversion of typical PLFA biomarkers for each group into biomass revealed that diatoms were the most abundant taxa, followed by coccolithophores and a minority of green algae (Fig. 2c, d, and e). The different taxa showed a similar response during the incubations, peaking at day 9. Diatom biomass rapidly increased after day 5 up to 0.50 ± 0.081 mg C L^{-1} at the peak of the bloom on day 9. The bloom declined to 0.11 ± 0.048 mg C L^{-1} at day 10 and remained low until the end of the incubations (Fig. 2c). A significant CO_2 effect could be detected in the post-bloom phase. The diatom biomass was significantly higher in the $2\times$ CO_2 and $3\times$ CO_2 treatments than in the $1\times$ CO_2 treatment, similar as for total phytoplankton (repeated measures ANOVA, $F\ (2,6) = 15.51$, $p < 0.005$) (Table 1). The CO_2 effect was mainly effective from day 12 to day 17. Coccolithophore biomass rapidly increased after day 5 and reached a peak of 0.19 ± 0.066 mg C L^{-1} at day 9. Coccolithophores declined after the bloom peak to concentrations of 0.047 ± 0.028 mg C L^{-1} at day 10 and remained low

Table 1. Average non-labelled biomass (mg C l^{-1}) and labelled biomass (µg C l^{-1}) of major phytoplankton groups and bacteria in the post-bloom phase (day 10–day 24) with p-values from post-hoc Bonferroni analyses after repeated measures ANOVA.

Organism	Value	1× CO_2	2× CO_2	3× CO_2	p 1×, 2×	p 1×, 3×	p 2×, 3×
Total phytoplankton	Biomass	0.13	0.15	0.17	**0.009**	**0.001**	0.22
	Labelled biomass	0.12	0.14	0.15	0.061	**0.010**	0.49
Diatoms	Biomass	0.066	0.085	0.090	**0.017**	**0.006**	0.96
	Labelled biomass	0.054	0.067	0.070	**0.017**	**0.004**	0.62
Coccolithophores	Biomass	0.030	0.032	0.034	1.00	0.86	1.00
	Labelled biomass	0.027	0.028	0.029	1.00	1.00	1.00
Green algae	Biomass	0.011	0.014	0.017	0.072	**0.003**	0.080
	Labelled biomass	0.0089	0.012	0.015	0.23	**0.011**	0.14
Bacteria	Biomass	0.086	0.11	0.12	**0.014**	**0.002**	0.34
	Labelled biomass	0.067	0.083	0.089	0.061	**0.013**	0.67

Values in bold are significant ($p < 0.05$)

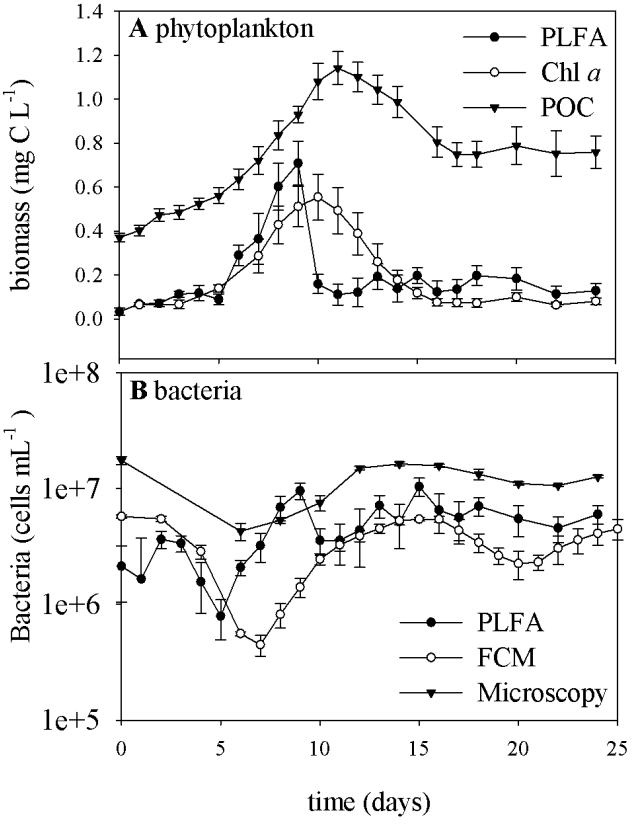

Fig. 3. Comparison of **(A)** phytoplankton biomass based on PLFA, Chl-*a*, and POC and **(B)** bacterial numbers based on PLFA, Flow Cytometry (FCM), and microscopy. Average and SD of all mesocosms are shown.

during the rest of the experiment (Fig. 2d). The development of coccolithophores in the post-bloom phase was independent of CO_2 (Table 1). The biomass of green algae was much lower than that of diatoms and coccolithophores with a maximum of 0.052 ± 0.0071 mg C L^{-1} at day 9 (Fig. 2e). The development of green algae in the post-bloom phase was dependent on CO_2 levels. Green algal biomass remained higher at elevated CO_2 levels, but only between the 1× and 3× CO_2 treatments were differences significant (repeated measures ANOVA, F (2,6) = 17.61, $p < 0.005$) (Table 1).

3.2 Bacterial dynamics

Bacterial dynamics showed more fluctuation during the experiment than phytoplankton (Fig. 2f). Initially, the bacteria biomass declined to a minimum at day 5 of 0.018 ± 0.0060 mg C L^{-1}. At the onset of the phytoplankton bloom, bacterial biomass started to increase. The bacterial biomass based on PLFA reached concentrations of 0.16 ± 0.051 mg C L^{-1} at the bloom peak on day 9 followed by a rapid decline to 0.056 ± 0.017 mg C L^{-1} at day 10 (Fig. 2f). After day 10, bacterial concentrations started to increase again to reach a second peak of 0.18 ± 0.030 mg C L^{-1} at day 18. In the post-bloom phase, the bacterial biomass was significantly higher at 3× CO_2 and 2× CO_2 compared to 1× CO_2 (repeated measures ANOVA, F (2,6) = 20.30, $p < 0.005$) (Table 1). The CO_2 effect was most pronounced between day 12 and day 17.

Bacterial cell abundances as determined by PLFA (this study, Fig. 2f), flow cytometry (FCM) (Paulino et al., 2008), and microscopy (Allgaier et al., 2008) are summarized in Fig. 3b. The range of cell numbers was similar for all methods ($10^9 - 10^{10}$ cells L^{-1}), indicating that bacteria were quantitatively retained on the GF/F filters used. However, the development of bacteria during the experiment differed

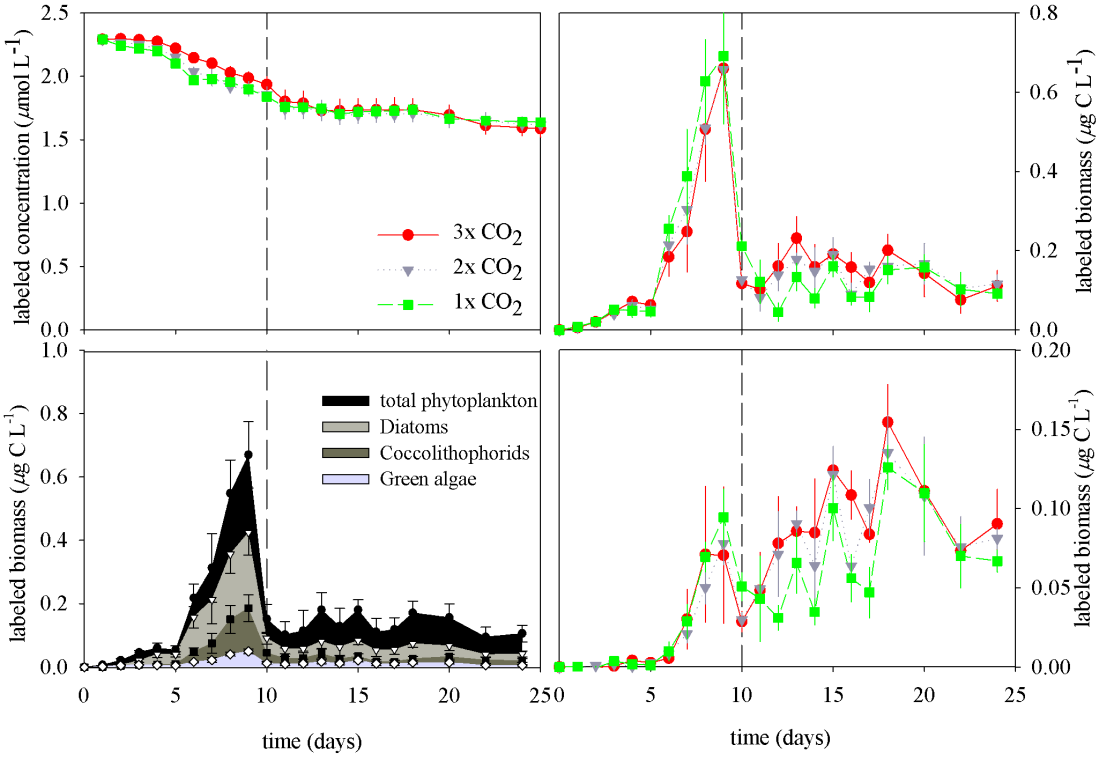

Fig. 4. Concentrations of ^{13}C labelled **(A)** DIC, **(B)** phytoplankton, phytoplankton groups **(C)**, and **(D)** bacteria. Average and SD of the three replicates are shown for (A–C) and average and SD of all mesocosm data are shown in (D).

for the three methods. The most striking difference occurred around the phytoplankton peak. While flow cytometry and microscopy revealed a minimum in bacterial abundance, PLFA based numbers showed a maximum in bacterial abundance.

3.3 Labelling

^{13}C-labeled DIC addition resulted in an increase of $\delta^{13}C$-DIC with 100.5 ± 11.9‰, from -1.73 ± 1.01‰ at day 0 up to 98.8 ± 12.5‰ at day 1. The large variation was caused by addition of different amounts of ^{13}C bicarbonate to individual mesocosms. During the experiment, the isotope ratio of DIC gradually decreased in all mesocosms to about 74‰ at day 25. Labelled DIC concentrations were 2.29 µmol C L^{-1} at day 1 and gradually decreased to 1.62 ± 0.05 µmol C L^{-1} at day 25 (Fig. 4a). The decrease in labelled DIC was independent of CO_2 levels. The loss of label from gas exchange between water and air was calculated only for the first 5 days, when biomass was still low. Label loss due to gas exchange was negligible for all treatments (<0.1%). A large part of labelled DIC was lost due to mixing with the deeper water layers. Assuming a mixing efficiency of 12% as calculated in Schulz et al. (2008), mixing with the deeper layers could explain 63 ± 10% of label loss.

The transfer from DIC to phytoplankton was very rapid; label enrichment in phytoplankton-specific PLFA was already detectable at day 1. The labelling of phytoplankton steadily increased from day 1 onwards and reached a maximum of 86.9 ± 10.4‰ at day 10, denoting that phytoplankton carbon reached steady-state with dissolved inorganic carbon. The ratios of phytoplankton isotope signature relative to DIC isotope signature, averaged over the last 10 days (day 15–24), are presented in Table 2. The average value was 1.04 ± 0.033 over all mesocosms, implying complete turnover of algal biomass during the experimental period. The development of label incorporation into phytoplankton matched with total phytoplankton dynamics; the labelled biomass was low in the first 5 days and then increased to a bloom peak at day 9 of 0.67 ± 0.10 µg C L^{-1}. The labelled biomass rapidly declined to 0.15 ± 0.046 µg C L^{-1} at day 10 and remained around this level until the end of the experiment (Fig. 4c). Labelled phytoplankton biomass in the post-bloom phase was significantly higher in the $3\times$ CO_2 treatment than in the $1\times$ CO_2 treatment, similar as for non-labelled phytoplankton biomass. The difference between the $1\times$ CO_2 and $2\times$ CO_2 treatments was not significant for labelled biomass in contrast to non-labelled biomass (repeated measures ANOVA, $F\ (2,6) = 11.51$, $p < 0.01$) (Table 1). The CO_2 effect was most pronounced from day 12 to day 17.

Table 2. Model parameters and steady-state ratios for each mesocosm ± standard deviation.

Mesocosm	r_{bac} (model)	f_{phyto} (model)	$\Delta\delta_{phytoplankton}/\Delta\delta_{DIC}$*	$\Delta\delta_{bacteria}/\Delta\delta_{phytoplankton}$*
7–1× CO_2	0.197 ± 0.0305	0.924 ± 0.0427	1.05	0.882
8–1× CO_2	0.197 ± 0.0291	0.908 ± 0.0434	1.03	0.857
9–1× CO_2	0.208 ± 0.0230	0.942 ± 0.0370	1.00	0.905
Average 1× CO_2	0.201 ± 0.00667	0.925 ± 0.0170	1.03 ± 0.023	0.8810 ± 0.0241
4–2× CO_2	0.208 ± 0.0267	0.921 ± 0.0356	1.01	0.885
5–2× CO_2	0.191 ± 0.0243	0.925 ± 0.0375	1.02	0.879
6–2× CO_2	0.230 ± 0.0516	0.888 ± 0.0513	1.10	0.851
Average 2× CO_2	0.209 ± 0.0195	0.911 ± 0.0203	1.04 ± 0.050	0.872 ± 0.0181
1–3× CO_2	0.270 ± 0.0475	0.860 ± 0.0371	1.04	0.857
2–3× CO_2	0.223 ± 0.0258	0.904 ± 0.0258	1.02	0.873
3–3× CO_2	0.192 ± 0.0303	0.920 ± 0.0410	1.08	0.864
Average 3× CO_2	0.228 ± 0.0395	0.895 ± 0.0308	1.04 ± 0.031	0.865 ± 0.00769

* average ratios over the last 10 days (day 15–24)

The labelling of the different phytoplankton groups was similar to labelling of total phytoplankton. Labelling of the different phytoplankton groups is presented as an average of all mesocosms in Fig. 4c. The CO_2 effects on the different phytoplankton groups were similar as for non-labelled biomass. Significant CO_2 effects were found in the post-bloom phase for diatoms, where biomass was higher in the 3× and 2× CO_2 treatments than in the 1× CO_2 incubations (repeated measures ANOVA, F (2,6) = 17.02, $p < 0.005$) and for green algae, where biomass was significantly higher in the 3× CO_2 treatment compared to the 1× CO_2 treatment (repeated measures ANOVA, F (2,6) = 10.84, $p = 0.01$) (Table 1). The specific growth rate during the bloom, as determined from label incorporation in biomass from day 5 to day 9, was highest for coccolithophores with a value of $0.76 \pm 0.11\,d^{-1}$, followed by green algae ($0.63 \pm 0.11\,d^{-1}$), and diatoms ($0.59 \pm 0.054\,d^{-1}$) (Fig. 5). Total phytoplankton growth rate was $0.64 \pm 0.075\,d^{-1}$. The growth rate of coccolithophores was significantly higher than the growth rates of green algae and diatoms (ANOVA, F (2,24) = 7.40, $p < 0.005$). Although the growth rates for each single group were not significantly affected by CO_2 treatment, it appeared that for coccolithophores, green algae and total phytoplankton, the growth rate was highest under current CO_2 levels (1× CO_2) (Fig. 5).

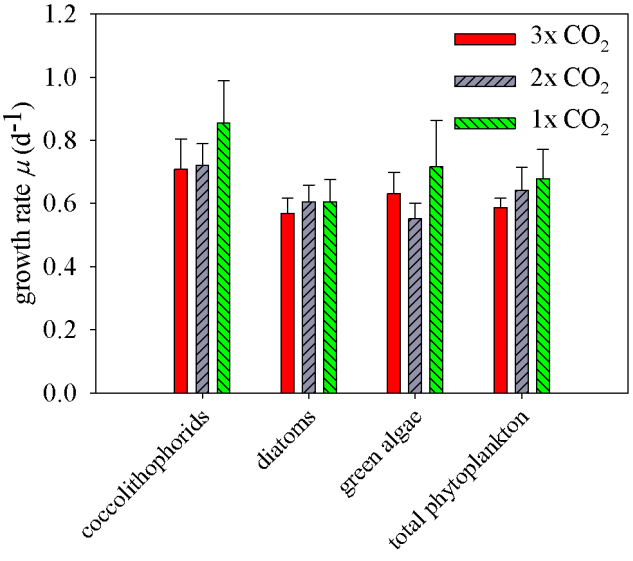

Fig. 5. Phytoplankton group-specific growth rates during the bloom period, day 5–9. Average and SD are shown.

The transfer of label to bacteria was much slower than the label transfer from DIC to phytoplankton. It was only at day 3 or 4, depending on the mesocosm, that enrichment could be detected in bacterial specific PLFA (Figs. 4d and 6). Average enrichment was 3.9 ± 3.1‰ on day 3 and 7.4 ± 5.8‰ on day 4. The isotope ratio steadily increased until 72.3 ± 8.8‰ at day 14, denoting isotope equilibrium. The ratios of bacterial isotope signature to phytoplankton isotope signature over the last 10 days (day 15–day 24) are presented in Table 2 for each mesocosm. The average ratio over all mesocosms was 0.87 ± 0.017 implying that 87% of the bacterial carbon was derived from recently fixed phytoplankton material. The other 13% was derived from non-labelled material. The dynamics of labelled bacteria were comparable with non-labelled bacteria; biomass was low in the first 5 days and showed some fluctuation in time. The peak in biomass was reached at day 18 with concentrations of $0.14 \pm 0.022\,\mu g\,C\,L^{-1}$ and declined afterwards (Fig. 4c). The labelled bacterial biomass was significantly higher in

the post-bloom phase in the $3\times CO_2$ treatment compared to $1\times CO_2$, but not in the $2\times CO_2$ treatment as for non-labelled biomass. The CO_2 effect was mainly present between day 12 and 17 (repeated measures ANOVA, $F\ (2,6) = 10.48$, $p < 0.05$) (Table 1).

3.4 Model

The transfer from phytoplankton to bacteria was quantified using a simple source-sink model (Eq. 1). The initial parameters range was 0–1 d^{-1} for both r_{bac} and f_{phyto}. The Bayesian approach produced a good fit to the data of all mesocoms (Fig. 6) and we were able to individually fit the parameters. Because of the large number of MCMC runs, reliable parameter distributions were obtained. The solid black lines are the model output, using the medians of the modelled bacterial ratios. The dark grey areas represent the 95% posterior limits of the model uncertainties. The light grey areas present the 95% posterior limits in predicting new observations (Malve et al., 2005, 2007). The turn-over rates for bacteria (r_{bac}) were $0.20 \pm 0.01\ d^{-1}$, $0.21 \pm 0.02\ d^{-1}$, and $0.23 \pm 0.04\ d^{-1}$, for $1\times CO_2$, $2\times CO_2$, $3\times CO_2$ treatments, respectively (Table 2). The fractions of bacterial carbon derived from phytoplankton (f_{phyto}) were $0.92 \pm 0.02\ d^{-1}$, $0.91 \pm 0.02\ d^{-1}$, $0.89 \pm 0.03\ d^{-1}$, for $1\times CO_2$, $2\times CO_2$, $3\times CO_2$ treatments, respectively (Table 2). The parameters were not significantly different for the different CO_2 treatments, but a trend with CO_2 concentrations could be observed. The value of f_{phyto} decreased with increasing CO_2 concentrations and the value of r_{bac} increased with increasing CO_2 concentrations.

3.5 Settled material

The isotope ratios of the material in the sediment traps were used to investigate whether sinking of organic matter from the upper layer to the deeper layer in the mesocosms was affected by the different treatments. The average isotope ratios of biomarker PLFA from the upper layer and the average isotope ratio of unlabeled PLFA (day 0) were used in the isotope mixing model to calculate the fraction in the traps derived from the upper layer. The fraction represents the exchange of material between upper and deeper layers. The fraction increased in time and was 0.29 ± 0.051 at day 4 and gradually increased to 0.90 ± 0.028 at day 16 for phytoplankton (Fig. 7a). Exchange was slightly faster in the beginning for bacterial PLFA than for phytoplankton PLFA. The fraction for bacteria was already 0.43 ± 0.12 at day 7, while it was only 0.33 ± 0.030 for phytoplankton. The exchange for bacteria gradually increased to 0.80 ± 0.077 at day 19 (Fig. 7b). Isotope mixing, which is an indication for sinking, was independent of CO_2 treatment.

4 Discussion

The combined use of stable isotopes and biomarkers provides a powerful tool to elucidate and quantify carbon fluxes in natural plankton communities (Boschker and Middelburg, 2002; Van Den Meersche et al., 2004; Pace et al., 2007). Here we applied the combined technique to determine the uptake of dissolved inorganic carbon by phytoplankton and subsequent transfer within the plankton community under different CO_2 levels. To our best knowledge, this is the first time that this approach is used to directly examine the transfer from phytoplankton to bacteria under changing CO_2 levels. The broad range of measured parameters (Riebesell et al., 2008) provided the opportunity to adequately describe the community response and to validate the use of PLFA as biomarkers. The high reproducibility of data between the different mesocosms resulted in robust outcomes of this experiment.

4.1 Phytoplankton and bacterial dynamics

The addition of inorganic nutrients initiated a phytoplankton bloom. The collapse of the bloom coincided with phosphate depletion at day 10 (Fig. 2a, h). The phytoplankton biomass at the bloom peak based on PLFA was $\sim 0.7\ mg\ C\ L^{-1}$, which corresponds to a moderate bloom. The peak in phytoplankton biomass as observed with PLFA occurred earlier (day 9) than the observed peak with chlorophyll-*a* (day 10) and POC (day 11) (Fig. 3a). The disagreement between bloom dynamics revealed with chlorophyll-*a* and PLFA is most likely due to function and structure of biomarkers and their turnover after cell death. PLFA are structural components of the cell membrane that rapidly decay after cell death. Consistent with pigment data (Riebesell et al., 2007; Schulz et al., 2008), PLFA data revealed that the bloom was dominated by prymnesiophytes (or coccolithophores) and diatoms (Fig. 2c, d, e). The group-specific dynamics, however, were different between pigment and PLFA analysis. In our study, no difference in diatom and coccolithophores succession was observed with PLFA. However, Riebesell et al. (2007), showed that diatoms peaked 1–2 days before coccolithophores, based on pigment analyses. The difference in succession of diatoms and coccolithophores with HPLC can be explained by earlier depletion of silicate (day 7) compared to phosphate (day 10) (Fig. 2h) (Schulz et al., 2008). Phytoplankton cell numbers for different groups were determined in this study with flow cytometry, but showed much more variability in time than PLFA and pigment analyses. POC reflects the total organic carbon pool including extracellular polymeric substances and phytoplankton detritus, which explains the ongoing build-up after the bloom peak (Fig. 3a) (Engel et al., 2002; Van den Meersche et al., 2004). Label incorporation into PLFA has proven to be a valuable tool to determine group-specific growth rates (Dijkman et al., 2009). High net growth rates were observed during the bloom with coccolithophores growing significantly faster than green algae and

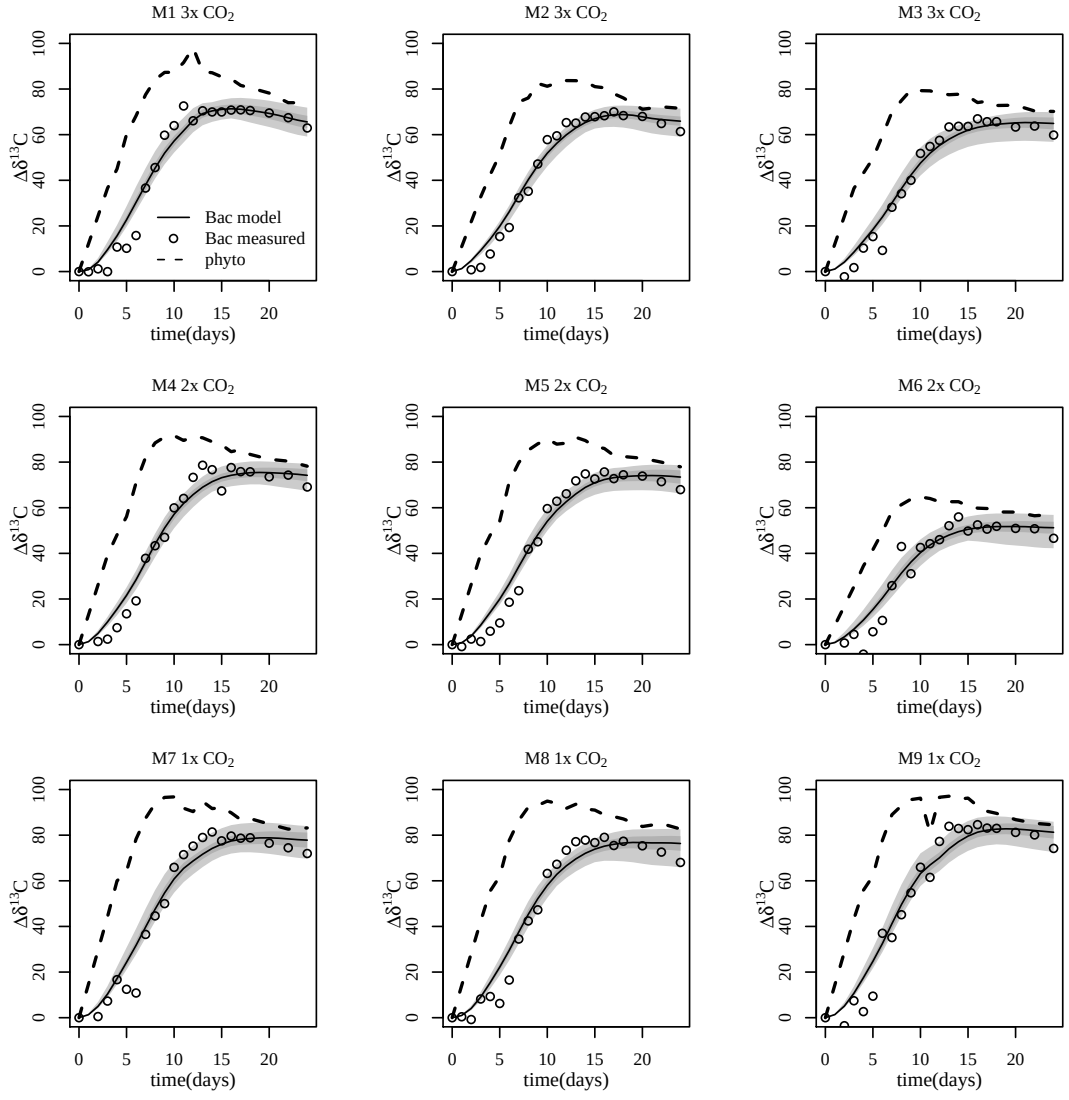

Fig. 6. Model simulations of ^{13}C transfer from phytoplankton to heterotrophic bacteria for individual mesocosms. Phytoplankton $\Delta\delta^{13}$C data (dashed line) are used as forcing function for model prediction (solid line; Bacteria (Bac) model) of bacterial $\Delta\delta^{13}$C data (open dots; Bac measured). Dark and light grey areas give 95% limits on model uncertainty and in predicting new observations, respectively (see text).

diatoms (Fig. 4). Our findings agree with the results obtained with the dilution method combined with pigment analysis during PeECE III, where prymnesiophytes growth rates were higher than diatom growth rates during the bloom (Suffrian et al., 2008).

The collapse of the phytoplankton bloom did not result in a noticeable increase in bacterial biomass and we did not observe a distinct heterotrophic phase in the second part of the experiment (Fig. 3). Bacterial dynamics correlated with phytoplankton dynamics during the phytoplankton bloom, with simultaneous higher concentrations of phytoplankton and bacteria. Overall, bacterial biomass increased during the experiment. In the PeECE III experiment, bacteria dynamics were also determined by microscopy (Allgaier et al., 2008) and flow cytometry (FCM) (Paulino et al., 2008). Bacterial dynamics based on PLFA biomarkers revealed a different pattern compared to dynamics based on microscopy and FCM. A striking difference between the different methods was between day 5 and 9. While microscopy and flow cytometry showed a minimum in bacterial numbers during the bloom build-up, PLFA showed a peak in bacterial abundance (Fig. 3b). This discrepancy can be explained by underestimation of bacterial number by FCM and microscopy due to shading by phytoplankton and a large number of phytoplankton-attached bacteria.

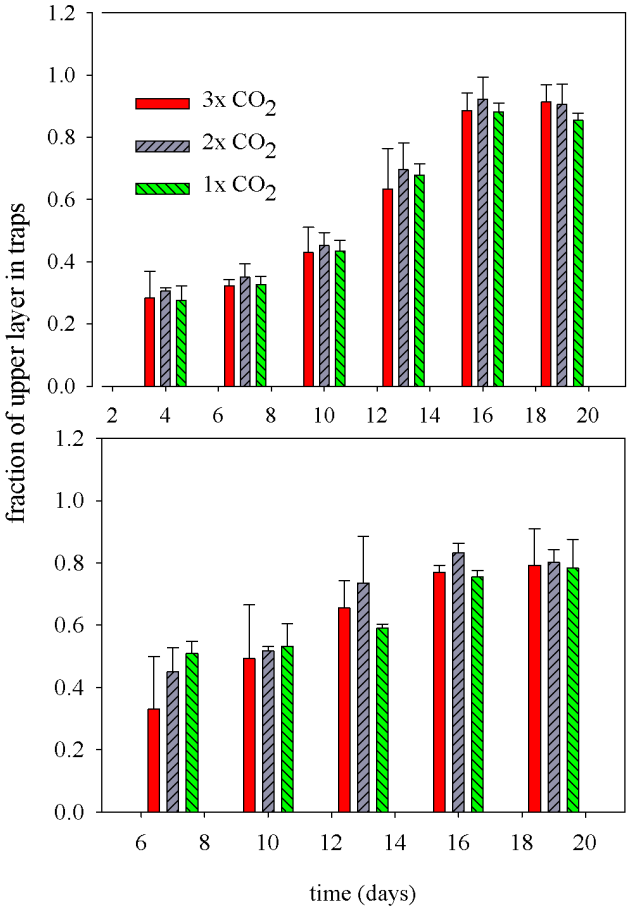

Fig. 7. The fractions in the sediment traps derived from the upper layer for **(A)** phytoplankton and **(B)** bacteria. Average and SD are shown for the triplicate mesocosms.

4.2 Phytoplankton-bacteria coupling

Phytoplankton derived organic matter is an important food-source for heterotrophic bacteria, resulting in a tight coupling between phytoplankton and bacterial production and abundance (Cole et al., 1988). Based on ^{13}C label dynamics, we observed a transfer from freshly produced phytoplankton material to heterotrophic bacteria. The label was detected in bacteria 2–3 days after incorporation in phytoplankton. At the end of the experiment 87% of bacterial carbon was derived from newly produced phytoplankton material (Fig. 4, Table 2). Overall the first part of the isotope curves mainly reflect uptake and turn-over dynamics, whereas the latter parts of the labelling experiment reflect food source clarification (Fry, 2006). To quantify turn-over dynamics and food source clarification in relation to CO_2 levels we applied a simple source-sink model as used in (Hamilton et al., 2004; Carpenter et al., 2005; Van Oevelen et al., 2006). In this model it is assumed that loss processes do not affect the isotope ratio (Figs. 2f, 4d). This is correct only if losses (e.g. bacterial respiration) operate on the bulk tissue. The sources however enrich the isotopic composition of the bacteria with the signature of the source compartment. We chose to assess the interactions with this simple model, with a few parameters, because it was possible to directly test the effect of CO_2 on the parameters of the system. In the first 7 days the model slightly overestimates the isotope ratio of bacteria (Fig. 6). The explanation for this is that f_{phyto} is in fact not constant in time; it will change in response to phytoplankton abundance.

The parameters obtained with our model are consistent with values described previously and obtained in other ways. Bacterial turn-over rates based on phytoplankton production ranged from 0.19 d^{-1} to 0.27 d^{-1} with an average of 0.21 d^{-1} in this study (Table 2). An average bacterial production of 20% of primary production was found in a literature survey by Cole et al. (1988). The fraction of bacterial biomass derived from phytoplankton products ranged from 0.86 to 0.94 with an average of 0.91, meaning that 91% of carbon in bacteria was coming from freshly produced phytoplankton material. The model derived dependency factors (f_{phyto}) are slightly higher than those based on the ratio $\Delta\delta^{13}C_{bac}/\Delta\delta^{13}C_{phyto}$ (Table 2), because of a slight decrease in bacterial isotope ratios at the end of the experiment. Dependency factors smaller than 1 indicate that bacteria also used the unlabeled algal carbon just fixed prior to incubation or used the unlabeled, background DOC pool, or the presence of an inactive bacteria population. Measurements of ^{13}C-DOC are required to test for these possibilities.

Few studies have used tracer dynamics and combined modelling to estimate carbon fluxes in natural plankton communities, making comparison limited. A similar experiment was conducted by Norman et al. (1995) who studied ^{13}C carbon transfer from phytoplankton to bacteria in an estuarine mesocosm experiment. At the end of their incubations, isotope ratios in bacteria were lower than those of POC, indicating that bacteria relied partly on not freshly produced material. A similar estimation of fluxes has been reported by Lyche et al. (1996) who traced ^{14}C in different size fractions as probes for primary and secondary production in a mesocosm study with lake communities. Their values were slightly different from ours (Table 2), with bacteria assimilation rates of 0.485 d^{-1} and a fraction of 0.704 derived from the phytoplankton. In contrast, Pace et al. (2007) observed almost complete dependence of heterotrophic (gram-positive) bacteria on phytoplankton in a clear-water lake. In their study, the whole lake was enriched with ^{13}C-DIC and traced into phytoplankton and bacteria, derived from 13C incorporation in PLFA biomarkers. Van Den Meersche et al. (2004) studied phytoplankton-bacteria interactions in a tracer experiment with estuarine water and also used PLFA biomarkers. They found a 100% dependency of bacteria on freshly produced phytoplankton material, revealed by similar isotope ratios in bacteria and phytoplankton PLFA at the end of the experiment.

We found a delay of 2–3 days in carbon transfer from phytoplankton to bacteria in all mesocosms (Fig. 6). The time lag is consistent with previous studies on phytoplankton-bacteria coupling. Duarte et al. (2005) observed a time-lag of 0–4 days between phytoplankton production and bacterial production in Southern Ocean plankton incubations. Ducklow et al. (1999) also observed lag periods of several days in bacterial response to phytoplankton bloom development in Southern Ocean plankton incubations. Van Den Meersche et al. (2004) observed a ∼1 day delay in labelling of bacteria compared to phytoplankton. Studies on biomass standing stocks of phytoplankton and bacteria during phytoplankton spring blooms also revealed some uncoupling and delay in response of bacteria to phytoplankton, varying from several days to weeks (Kirchman et al., 1994; Lochte et al., 1997), while a close coupling was observed by Lancelot and Billen (1984). There are several possible explanations for these "lags" or "uncoupling". The most obvious explanation is the presence of unlabeled DOM at the start of the experiment, which is later replenished by labelled DOM. DOM release by phytoplankton can occur passively (leakage and viral lysis) or actively under nutrient starvation (Van Den Meersche et al., 2004). Possibly, DOM release was low in the first part of the experiment (before and during the bloom) because it occurred mainly passively and the major DOM release took place during the bloom collapse, although this was not reflected in standing-stock measurements of DOC (Schulz et al., 2008). Other explanations that concern more the physiological state of the bacteria have been summarized by Ducklow et al. (1999). They suggested that most, if not all, marine bacteria exist predominantly in a state of dormancy, under severe carbon, phosphate, and/or energy starvation. Another possibility is that the apparent lag phase reflects logistic (s-shaped) growth curves. A third scenario concerns the hypothetical existence of non-dividing subpopulations of cells which are progressively overgrown by the growing populations. The high dependency of bacteria on phytoplankton (Table 2) and the small increase in DOM standing stocks (Schulz et al., 2008) during the experiment indicate a strong coupling between phytoplankton and heterotrophic bacteria. Probably there was strong grazing pressure on bacteria that kept the bacterial standing stock low. Bacterivory was indeed high during the experiment as determined by measuring uptake of fluorescent labelled bacteria by protists (Tanaka and Løvdal, unpublished data, 2005).

4.3 Sinking of fresh produced material

The establishment of the halocline separated the surface layer and deep layer and the sediment traps were located in the deep layer. Unfortunately, windy conditions caused mixing of the water in the mesocosms and resuspension of already settled material, especially on day 12 when a heavy storm occurred (Schulz et al., 2008). These circumstances made it difficult to use absolute numbers of phytoplankton and bacterial biomass in the sediment traps. Consequently we limit our analysis to isotope ratios and to the first 12 days, which can still give some insight in sinking of freshly produced material. Mixing between the upper and deeper layer was not so important, since at day 10 only about half of the material in the sediment traps was derived from the upper layer (Fig. 7). An interesting observation is that bacteria derived material settled more rapidly than phytoplankton material. Close relationships exist between bacteria and detritus. Bacteria rapidly colonize detritus and enhance further aggregation of detritus and subsequent sinking (e.g. Biddanda and Pomeroy, 1988). Because of turnover of PLFA after phytoplankton death, the detritus will contain less phytoplankton PLFA and there is thus a preferential sinking of bacteria over phytoplankton (as determined with PLFA), which could be another explanation for the low standing stock in bacteria (Figs. 2f and 3b). Because POC consists both of living biomass and detritus, the stable isotope ratio of POC would be a better source for estimating organic matter dynamics. During this study we did not measure ^{13}C content of POC, so we could only use phytoplankton PLFA.

4.4 CO_2 effects and implications for ocean acidification

In this study, we aimed to advance our understanding of the effect of elevated pCO_2 levels on phytoplankton and bacterial dynamics and on the interactions between them. Furthermore we aimed to gain insight on the effect of CO_2 on sinking of freshly produced material. Our results clearly show an effect of CO_2 on total and labelled standing stocks of bacteria and phytoplankton in the post-bloom phase, but not on carbon transfer from DIC to phytoplankton and subsequently bacteria. Unfortunately, during the post-bloom phase a heavy storm mixed the mesocosms, making it difficult to quantify settling processes. The phytoplankton bloom was independent of CO_2 concentrations in this study (Figs. 2 and 4). These results agree with other results obtained in PeECE III on phytoplankton bloom development. Phytoplankton bloom development based on pigments (Riebesell et al., 2007; Schulz et al., 2008), flow cytometry (Paulino et al., 2008), and particulate organic carbon (Schulz et al., 2008) was also found to be CO_2 independent during the PeECE III mesocosm experiment. Previous CO_2 enrichment mesocosm studies also showed little effect on particulate organic matter production, although the effect of CO_2 is species dependent. In PeECE I, some phytoplankton groups like coccolithophores were sensitive to changes in CO_2, where other groups like diatoms were not (Delille et al., 2005; Engel et al., 2005).

Interestingly, we did observe CO_2 related effects in the post-bloom phase of the experiment. Green algae and diatoms seemed to benefit from increased pCO_2 as their biomass was significantly higher under high CO_2 levels in the post-bloom phase (Fig. 2, Table 1). Current CO_2 levels are generally considered to be a non-limiting resource for

diatoms and green algae, because they have efficient carbon concentrating mechanisms (CCMs) (Giordano et al., 2005). But the operation of these mechanisms requires energy, so when energy becomes limited, higher CO_2 concentrations can be beneficial. In a recent study from Feng et al. (2009), diatom abundance increased with increasing pCO_2 in shipboard community incubations. Moreover, Egge et al. (2009) reported higher total community primary production rates in the post-bloom phase of the PeECE III experiments in high CO_2 treatments (Fig. 1).

We found no indication of enhanced sinking of phytoplankton at increasing CO_2 levels based on isotope ratios in the sediment traps (Fig. 7). However, the results should be interpreted with caution. Sinking of freshly produced material would mainly occur during and after the bloom collapse and we do not have reliable sediment trap data for that period due to the storm event. An enhanced carbon consumption was based on DIC budgets (Riebesell et al., 2007; Bellerby et al., 2008), but was not reflected in standing stocks of biological material. The concentrations of TEP (Egge et al., 2009), POC and DOC were independent of CO_2 (Fig. 1) (Schulz et al., 2008). Riebesell et al. (2007) suggested that the discrepancy may have been caused by an enhanced particle sinking. Unfortunately, our sediment trap data could not be used to confirm or falsify this hypothesis.

The development of bacterial biomass showed a similar response to CO_2 as phytoplankton, with a significantly higher biomass at higher CO_2 in the post-bloom phase compared to present pCO_2 levels (Figs. 2f and 4d, Table 1). In the post-bloom phase, our results concerning bacterial dynamics differ from those of other bacteria results from PeECE III studies. No differences in bacterial abundance under the different CO_2 levels were observed with flow cytometry and with microscopy (Allgaier et al., 2008; Paulino et al., 2008). Previous studies have shown that the response of heterotrophic bacteria to changing CO_2 levels is linked to phytoplankton rather than being a direct effect of pH or CO_2 (e.g. Grossart et al., 2006). The increased biomass at higher pCO_2 could be a direct result of increased phytoplankton biomass at higher pCO_2 in the post-bloom phase. We did not observe enhanced coupling between phytoplankton and bacteria under higher pCO_2 with the isotope transfer model during the bloom (Fig. 6, Table 2). Due to label saturation, the coupling could only be studied before and during the bloom and not in the post-bloom phase. Phytoplankton carbon exudation generally increases at the end of a phytoplankton bloom when nutrients become limited and a CO_2 effect is thus more likely to occur in this phase (Van den Meersche et al., 2004; Engel et al., 2004a). For future CO_2 studies on phytoplankton-bacteria coupling, it can be helpful to use nutrient-limited plankton incubations or to add carbon tracer in the post-bloom phase.

Acknowledgements. The authors gratefully acknowledge the staff of the Espegrend Marine Biological Station, University Bergen, in particular T. Sørlie and A. Aadnesen, and the Bergen Marine Research infrastructure (RI) for helping organize and set up the mesocosm experiment. PeECEIII team members are thanked for the stimulating environment and for providing access to data. We thank Ulysses S. Ninnemann for technical support on DIC analyses. Marco Houtekamer and Pieter van Rijswijk are greatly acknowledged for their work on PLFA extractions and analyses. We thank Dick van Oevelen, Frederik de Laender, Eric Boschker, and Jacco Kromkamp for their help with data analyses. Thanks to Francesc Montserrat and Peter Herman for helping with statistical analyses. This study received financial support from the European Project on Ocean Acidification (EPOCA, FP7, 2211384), the Marine Ecosystem Evolution in a Changing Environment project (MEECE, FP7, 212085), the Marine Ecosystem Response to a Changing Climate (MERCLIM, NFR, 184860) and the Darwin Center for Biogeosciences supported by the Netherlands Organisation for Scientific Research. This is publication number 4909 of the Netherlands Institute of Ecology (NIOO-KNAW).

Edited by: S. Bouillon

References

Allgaier, M., Riebesell, U., Vogt, M., Thyrhaug, R., and Grossart, H.-P.: Coupling of heterotrophic bacteria to phytoplankton bloom development at different pCO_2 levels: a mesocosm study, Biogeosciences, 5, 1007–1022, doi:10.5194/bg-5-1007-2008, 2008.

Arrigo, K. R.: Carbon cycle – Marine manipulations, Nature, 450, 491–492, 2007.

Bellerby, R. G. J., Schulz, K. G., Riebesell, U., Neill, C., Nondal, G., Heegaard, E., Johannessen, T., and Brown, K. R.: Marine ecosystem community carbon and nutrient uptake stoichiometry under varying ocean acidification during the PeECE III experiment, Biogeosciences, 5, 1517–1527, doi:10.5194/bg-5-1517-2008, 2008.

Biddanda, B. A. and Pomeroy, L. R.: Microbial aggregation and degradation of phytoplankton-derived detritus in seawater. 1. Microbial succession, Mar. Ecol.-Prog. Ser., 42, 79–88, 1988.

Bligh, E. G. and Dyer, W. J.: A rapid method of total lipid extraction and purification, Can. J. Biochem. Phys., 37, 911–917, 1959.

Boschker, H. T. S. and Middelburg, J. J.: Stable isotopes and biomarkers in microbial ecology, Fems Microbiol. Ecol., 40, 85–95, 2002.

Boschker, H. T. S., Nold, S. C., Wellsbury, P., Bos, D., de Graaf, W., Pel, R., Parkes, R. J., and Cappenberg, T. E.: Direct linking of microbial populations to specific biogeochemical processes by ^{13}C-labelling of biomarkers, Nature, 392, 801–805, 1998.

Brinch Iversen, J. and King, G. M.: Effects of substrate concentration, growth-state, and oxygen availability on relationships among bacterial carbon, nitrogen and phospholipid phosphorus-content, Fems Microbiol. Ecol., 74, 345–355, 1990.

Carpenter, S. R., Cole, J. J., Pace, M. L., Van de Bogert, M., Bade, D. L., Bastviken, D., Gille, C. M., Hodgson, J. R., Kitchell, J. F., and Kritzberg, E. S.: Ecosystem subsidies: Terrestrial support of aquatic food webs from ^{13}C addition to contrasting lakes, Ecology, 86, 2737–2750, 2005.

Cole, J. J., Findlay, S., and Pace, M. L.: Bacterial production in fresh and saltwater ecosytstems – A cross-system overview, Mar. Ecol.-Prog. Ser., 43, 1–10, 1988.

Delille, B., Harlay, J., Zondervan, I., Jacquet, S., Chou, L., Wollast, R., Bellerby, R. G. J., Frankignoulle, M., Borges, A. V., Riebesell, U., and Gattuso, J. P.: Response of primary production and calcification to changes of pCO_2 during experimental blooms of the coccolithophorid Emiliania huxleyi, Global Biogeochem. Cy., 19(14), Gb2023, doi:10.1029/2004gb002318, 2005.

Dijkman, N. A. and Kromkamp, J. C.: Phospholipid-derived fatty acids as chemotaxonomic markers for phytoplankton: application for inferring phytoplankton composition, Mar. Ecol.-Prog. Ser., 324, 113–125, 2006.

Dijkman, N., Boschker, H., Middelburg, J., and Kromkamp, J. C.: Group-specific primary production based on stable-isotope labelling of phospholipid-derived fatty acids, Limnol. Oceanogr.-Meth., 7, 612–625, 2009.

Duarte, C. M., Agusti, S., Vaque, D., Agawin, N. S. R., Felipe, J., Casamayor, E. O., and Gasol, J. M.: Experimental test of bacteria-phytoplankton coupling in the Southern Ocean, Limnol. Oceanogr., 50, 1844–1854, 2005.

Ducklow, H., Carlson, C., and Smith, W.: Bacterial growth in experimental plankton assemblages and seawater cultures from the Phaeocystis antarctica bloom in the Ross Sea, Antarctica, Aquat. Microb. Ecol., 19, 215–227, 1999.

Egge, J. K., Thingstad, T. F., Larsen, A., Engel, A., Wohlers, J., Bellerby, R. G. J., and Riebesell, U.: Primary production during nutrient-induced blooms at elevated CO_2 concentrations, Biogeosciences, 6, 877–885, doi:10.5194/bg-6-877-2009, 2009.

Engel, A., Delille, B., Jacquet, S., Riebesell, U., Rochelle-Newall, E., Terbruggen, A., and Zondervan, I.: Transparent exopolymer particles and dissolved organic carbon production by Emiliania huxleyi exposed to different CO_2 concentrations: a mesocosm experiment, Aquat. Microb. Ecol., 34, 93–104, 2004a.

Engel, A., Goldthwait, S., Passow, U., and Alldredge, A.: Temporal decoupling of carbon and nitrogen dynamics in a mesocosm diatom bloom, Limnol. Oceanogr., 47, 753–761, 2002.

Engel, A., Thoms, S., Riebesell, U., Rochelle-Newall, E., and Zondervan, I.: Polysaccharide aggregation as a potential sink of marine dissolved organic carbon, Nature, 428, 929–932, 2004b.

Engel, A., Zondervan, I., Aerts, K., Beaufort, L., Benthien, A., Chou, L., Delille, B., Gattuso, J. P., Harlay, J., Heemann, C., Hoffmann, L., Jacquet, S., Nejstgaard, J., Pizay, M. D., Rochelle-Newall, E., Schneider, U., Terbrueggen, A., and Riebesell, U.: Testing the direct effect of CO_2 concentration on a bloom of the coccolithophorid Emiliania huxleyi in mesocosm experiments, Limnol. Oceanogr., 50, 493–507, 2005.

Feng, Y. Y., Hare, C. E., Leblanc, K., Rose, J. M., Zhang, Y. H., DiTullio, G. R., Lee, P. A., Wilhelm, S. W., Rowe, J. M., Sun, J., Nemcek, N., Gueguen, C., Passow, U., Benner, I., Brown, C., and Hutchins, D. A.: Effects of increased pCO_2 and temperature on the North Atlantic spring bloom. I. The phytoplankton community and biogeochemical response, Mar. Ecol.-Prog. Ser., 388, 13–25, doi:10.3354/meps08133, 2009.

Fogg, G. E.: The ecological significance of extracellular products of phytoplankton photosynthesis, Bot. Mar., 26, 3–14, 1983.

Fry, B.: Stable isotope ecology, Springer, 2006.

Gelman, A.: Inference and monitoring convergence, in: Markov Chain Monte Carlo in Practice, edited by: Gilks, W. R., Richardson, S., and Spiegelhalter, D. J., London, UK, Chapman & Hall, 131–140, 1996.

Giordano, M., Beardall, J., and Raven, J. A.: CO_2 concentrating mechanisms in algae: Mechanisms, environmental modulation, and evolution, Annu. Rev. Plant Biol., 56, 99–131, 2005.

Grossart, H. P., Allgaier, M., Passow, U., and Riebesell, U.: Testing the effect of CO_2 concentration on the dynamics of marine heterotrophic bacterioplankton, Limnol. Oceanogr., 51, 1–11, 2006.

Hamilton, S. K., Tank, J. L., Raikow, D. F., Siler, E. R., Dorn, N. J., and Leonard, N. E.: The role of instream vs allochthonous N in stream food webs: modelling the results of an isotope addition experiment, J. N. Am. Benthol. Soc., 23, 429–448, 2004.

Kirchman, D. L., Ducklow, H. W., McCarthy, J. J., and Garside, C.: Biomass and nitrogen uptake by heterotrophic bacteria during the spring phytoplankton bloom in the North-Atlantic ocean, Deep-Sea Res. Pt. I, 41, 879–895, 1994.

Kritzberg, E. S., Cole, J. J., Pace, M. L., Granéli, W., and Bade, D. L.: Autochthonous versus Allochthonous Carbon Sources of Bacteria: Results from Whole-Lake ^{13}C Addition Experiments, Limnol. Oceanogr., 49, 588–596, 2004.

Lancelot, C. and Billen, G.: Activity of heterotrophic bacteria and its coupling to primary production during the spring phytoplankton bloom in the southern bight of the North-sea, Limnol. Oceanogr., 29, 721–730, 1984.

Larsson, U. and Hagstrom, A.: Phytoplankton Exudate Release as an Energy-Source for the Growth of Pelagic Bacteria, Mar. Biol., 52, 199–206, 1979.

Lee, S. and Fuhrman, J. A.: Relationships between biovolume and biomass of naturally derived marine bacterioplankton, Appl. Environ. Microb., 53, 1298–1303, 1987.

Lochte, K., Bjornsen, P. K., Giesenhagen, H., and Weber, A.: Bacterial standing stock and production and their relation to phytoplankton in the Southern Ocean, Deep-Sea Res. Pt. II, 44, 321–340, 1997.

Lyche, A., Andersen, T., Christoffersen, K., Hessen, D. O., Hansen, P. H. B., and Klysner, A.: Mesocosm tracer studies. 2. The fate of primary production and the role of consumers in the pelagic carbon cycle of a mesotrophic lake, Limnol. Oceanogr., 41, 475–487, 1996.

Malve, O., Laine, M., and Haario, H.: Estimation of winter respiration rates and prediction of oxygen regime in a lake using Bayesian inference, Ecol. Model., 182, 183–197, doi:10.1016/j.ecolmodel.2004.07.020, 2005.

Malve, O., Laine, M., Haario, H., Kirkkala, T., and Sarvala, J.: Bayesian modelling of algal mass occurrences – using adaptive MCMC methods with a lake water quality model, Environ. Modell. Softw., 22, 966–977, doi:10.1016/j.envsoft.2006.06.016, 2007.

Middelburg, J. J., Barranguet, C., Boschker, H. T. S., Herman, P. M. J., Moens, T., and Heip, C. H. R.: The fate of intertidal microphytobenthos carbon: An in situ C-13-labeling study, Limnol. Oceanogr., 45, 1224–1234, 2000.

Norrman, B., Zweifel, U. L., Hopkinson, C. S., and Fry, B.: Production and utilization of dissolved organic carbon during an experimental diatom bloom, Limnol. Oceanogr., 40, 898–907, 1995.

Pace, M. L., Carpenter, S. R., Cole, J. J., Coloso, J. J., Kitchell, J. F., Hodgson, J. R., Middelburg, J. J., Preston, N. D., Solomon, C. T., and Weidel, B. C.: Does terrestrial organic carbon subsidize the planktonic food web in a clear-water lake?, Limnol. Oceanogr.,

52, 2177–2189, 2007.

Paulino, A. I., Egge, J. K., and Larsen, A.: Effects of increased atmospheric CO_2 on small and intermediate sized osmotrophs during a nutrient induced phytoplankton bloom, Biogeosciences, 5, 739–748, doi:10.5194/bg-5-739-2008, 2008.

Press, W., Teukolsky, S., Vetterling, W., and Flannery, B.: Numerical recipes: the art of scientific computing, Cambridge Univ. Pr., 2007.

Riebesell, U., Wolfgladrow, D. A., and Smetacek, V.: Carbon-dioxide limitation of marine-phytoplankton growth-rates, Nature, 361, 249–251, 1993.

Riebesell, U., Schulz, K. G., Bellerby, R. G. J., Botros, M., Fritsche, P., Meyerhöfer, M., Neill, C., Nondal, G., Oschlies, A., Wohlers, J., and Zöllner, E.: Enhanced biological carbon consumption in a high CO_2 ocean, Nature, 450, 545–549, 2007.

Riebesell, U., Bellerby, R. G. J., Grossart, H.-P., and Thingstad, F.: Mesocosm CO_2 perturbation studies: from organism to community level, Biogeosciences, 5, 1157–1164, doi:10.5194/bg-5-1157-2008, 2008.

Rivkin, R. B. and Legendre, L.: Biogenic carbon cycling in the upper ocean: Effects of microbial respiration, Science, 291, 2398–2400, 2001.

Sabine, C. L., Feely, R. A., Gruber, N., Key, R. M., Lee, K., Bullister, J. L., Wanninkhof, R., Wong, C. S., Wallace, D. W. R., Tilbrook, B., Millero, F. J., Peng, T. H., Kozyr, A., Ono, T., and Rios, A. F.: The oceanic sink for anthropogenic CO_2, Science, 305, 367–371, 2004.

Schulz, K. G., Riebesell, U., Bellerby, R. G. J., Biswas, H., Meyerhöfer, M., Müller, M. N., Egge, J. K., Nejstgaard, J. C., Neill, C., Wohlers, J., and Zöllner, E.: Build-up and decline of organic matter during PeECE III, Biogeosciences, 5, 707–718, doi:10.5194/bg-5-707-2008, 2008.

Soetaert, K. and Petzoldt, T.: FME: A Flexible Modelling Environment for inverse modelling, sensitivity, identifiability, monte carlo analysis, R package version, 1, 2009.

Soetaert, K., Petzoldt, T., and Setzer, R. W.: deSolve: General solvers for initial value problems of ordinary differential equations (ODE), partial differential equations (PDE) and differential algebraic equations (DAE), R package version, 1, 2009.

Suffrian, K., Simonelli, P., Nejstgaard, J. C., Putzeys, S., Carotenuto, Y., and Antia, A. N.: Microzooplankton grazing and phytoplankton growth in marine mesocosms with increased CO_2 levels, Biogeosciences, 5, 1145–1156, doi:10.5194/bg-5-1145-2008, 2008.

Tanaka, T., Thingstad, T. F., Løvdal, T., Grossart, H.-P., Larsen, A., Allgaier, M., Meyerhöfer, M., Schulz, K. G., Wohlers, J., Zöllner, E., and Riebesell, U.: Availability of phosphate for phytoplankton and bacteria and of glucose for bacteria at different pCO_2 levels in a mesocosm study, Biogeosciences, 5, 669–678, doi:10.5194/bg-5-669-2008, 2008.

Thingstad, T., Bellerby, R., Bratbak, G., Børsheim, K., Egge, J., Heldal, M., Larsen, A., Neill, C., Nejstgaard, J., and Norland, S.: Counterintuitive carbon-to-nutrient coupling in an Arctic pelagic ecosystem, Nature, 455, 387–390, 2008.

Van den Meersche, K., Middelburg, J. J., Soetaert, K., van Rijswijk, P., Boschker, H. T. S., and Heip, C. H. R.: Carbon-nitrogen coupling and algal-bacterial interactions during an experimental bloom: Modeling a ^{13}C tracer experiment, Limnol. Oceanogr., 49, 862–878, 2004.

Van den Meersche, K., Soetaert, K., and Middelburg, J. J.: A Bayesian compositional estimator for microbial taxonomy based on biomarkers, Limnol. Oceanogr.-Meth., 6, 190–199, 2008.

Van Oevelen, D., Moodley, L., Soetaert, K., and Middelburg, J. J.: The trophic significance of bacterial carbon in a marine intertidal sediment: Results of an in situ stable isotope labelling study, Limnol. Oceanogr., 51, 2349–2359, 2006.

Zeebe, R. E. and Wolf-Gladrow, D. A.: CO_2 in Seawater: Equilibrium, Kinetics, Isotopes, Elsevier Science, 2001.

Zhang, J., Quay, P. D., and Wilbur, D. O.: Carbon-isotope fractionation during gas-water exchange and dissolution of CO_2, Geochim. Cosmochim. Ac., 59, 107–114, 1995.